

Integrated Multimaterial Fibres for Self-Monitored Optical Transport

RLE Groups

Photonic Bandgap Fibers and Devices Group, ab initio Physics Group

Academic and Research Staff

Mehmet Bayindir, Ayman F. Abouraddy, John D. Joannopoulos, and Yoel Fink

Graduate Students

Ofer Shapira, Dursen Saygin-Hinczewski, and Jeff Viens

Sponsors

DARPA, the ARO, the ONR, the US DOE, and the ISN.

The ability to integrate a multiplicity of distinct functional elements into a single device structure enables the realization of systems with higher-level functionality. Here we report on the design and fabrication of a fiber device structure which contains integrated optical, electrical and thermal elements for self monitored optical transport. The fibers comprise an optical transmission element which is a hollow-core multilayer cylindrical photonic bandgap (PBG) structure designed to guide high power radiation at 10.6 microns along the fiber axis. Multiple thermal-detection elements are placed in the vicinity of the hollow core for the purpose of temperature monitoring along the entire fiber length. Metal wires bridged by a semiconductor layer extend along the length of the fiber and deliver an electrical response to the fiber ends upon change in the fiber temperature. The multimaterial fiber, which contains a polymer insulator, a binary large bandgap semiconductor, a quaternary narrow bandgap semiconductor, and metallic elements, is drawn at high speeds from a single fiber preform to produce extended lengths of optically and thermally functional fibers. The exponential dependence on temperature of the electrical conductivity of the semiconducting material allows for the discrimination - in real time - between normal transmission conditions and those which are indicative of localized defect formation, thus enabling for the first time a self monitoring high power optical transmission line for failure prediction and prevention.

Published

[1] Y. Fink et al., "A Dielectric Omnidirectional Reflector," *Science* 282: 1679 (1998).

[2] B. Temelkuran et al., "Wavelength-Scalable Hollow Optical Fibres with Large Photonic Bandgaps for CO₂ Laser Transmission," *Nature* 420: 650 (2002).

[3] M. Bayindir, et al., "Metal-Insulator-Semiconductor Optoelectronic Fibres," *Nature* 431: 826 (2004).

Accepted for Publication

[4] M. Bayindir, et al., "Integrated Fibres for Self-Monitored Optical Transport," *Nature Materials*, forthcoming (2005).

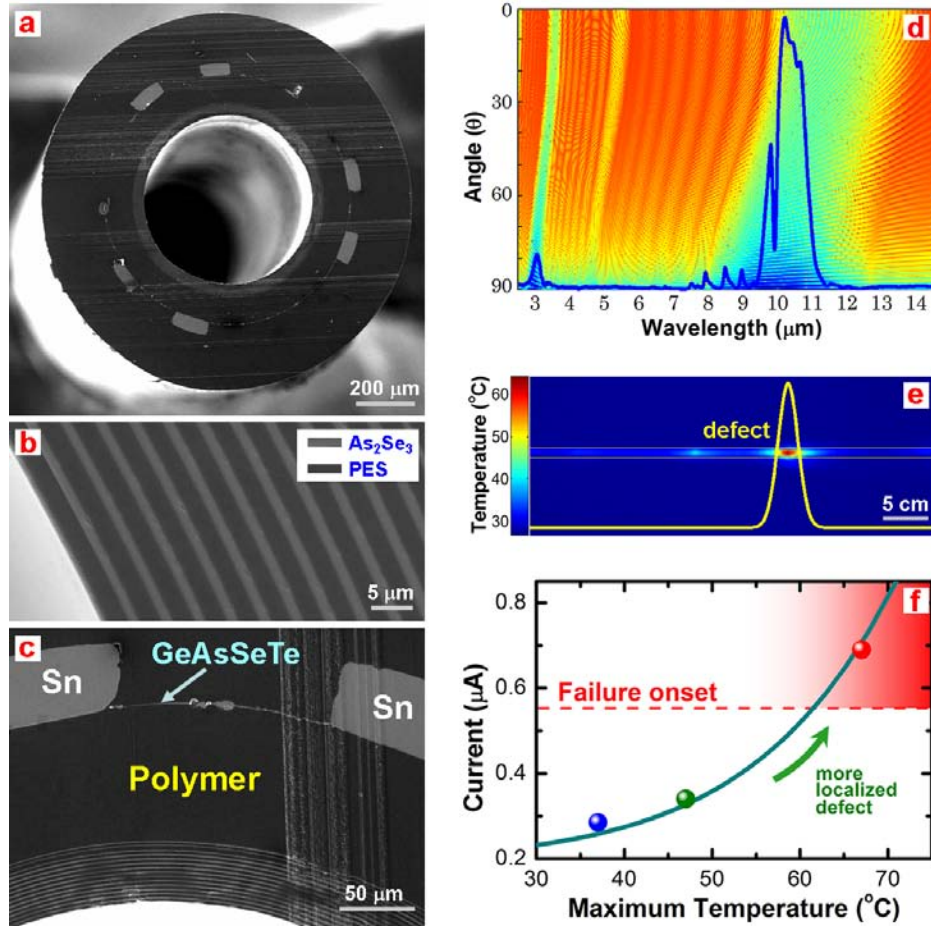


Figure 1: SEM micrographs of the integrated fiber; (a) the entire cross section, (b) the metal-semiconductor-metal (MSM) heat sensor and (c) the cylindrical omnidirectional Bragg mirror. (d) Calculated band diagram of cylindrical multilayer photonic band gap structure, and measured broad-band transmission spectrum (blue solid line). (e) Thermal photograph of a fiber containing a single localized defect and temperature distribution along the fiber (yellow solid line). (f) Calculated current as a function of the maximum temperature along the fiber for a constant dissipated power.

LARGE-SCALE OPTICAL-FIELD MEASUREMENTS WITH GEOMETRIC FIBRE CONSTRUCTS

Academic and Research Staff

Ayman F. Abouraddy, Mehmet Bayindir, Jerimy Arnold, John D. Joannopoulos, and Yoel Fink

Graduate Students

Ofer Shapira, Fabien Sorin, and Dursen Saygin-Hinczewski

Measurements of optical fields are typically performed using sequential arrangements of optical components such as lenses, filters, beam splitters in conjunction with planar arrays of point detectors placed on a common axis; both the human eye and the photographic camera are examples of such systems. While the specifics may vary from system to system, all are constrained in terms of size, weight, durability and field of view around the optical axis. Here, a new, geometric approach to optical field measurements is presented that lifts some of the fundamental limitations associated with conventional measurement systems and, moreover, enables access to optical information on unprecedented length and volume scales. Tough polymeric photodetecting fibres drawn from a perform are woven into light-weight, low-optical-density, two- and three-dimensional constructs that measure the basic attributes of electromagnetic fields on very large areas. The precise geometric construct is tailored to address specific measurement requirements and, in particular, does not necessitate an optical axis. First, we show how a planar geometry may reconstruct an arbitrary optical field intensity distribution using a tomographic algorithm. Non-interferometric lensless imaging is then achieved using a two-plane arrangement that reconstructs both the amplitude and the phase distributions of an incoming field, enabling one to readily reconstruct the object from which the field originally emanated. Finally, a three-dimensional spherical geometry is used to demonstrate an omnidirectional light detection system capable of discerning the direction of illumination over 4π steradians. Hence, the problem of optical field measurement is transformed from one involving the choice and placement of lenses and detector arrays to that of designing geometrical constructions of polymeric, light-sensitive fibres.

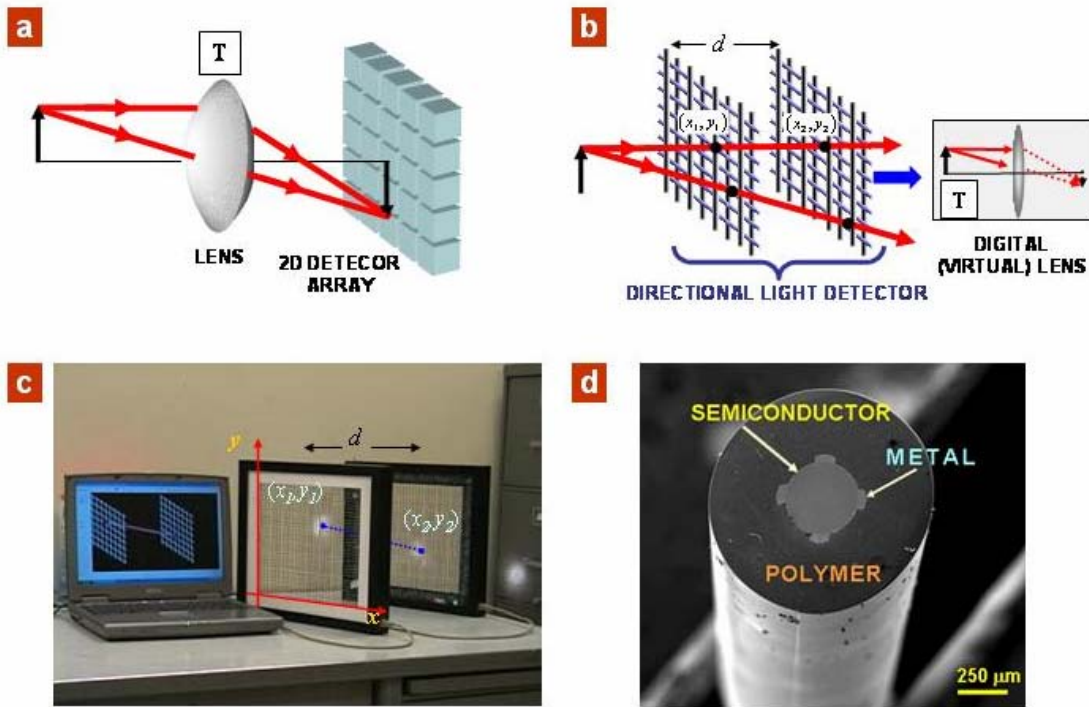


Figure 1 Photodetecting fiber webs. **a**, A typical optical imaging configuration. A lens implements an optical transformation T that results in mapping incoming rays to outgoing ones. A 2D detector array then detects the incident intensity distribution. **b**, Two transparent, planar detector arrays constitute a directional light detector. Given the location and direction of the ray, one may implement the optical transformation of the lens T digitally on a computer. **c**, A physical implementation of a directional light detector consisting of two planar fiber webs, displaying the path of a ray of white light in three dimensions. The two planar fiber webs detect the positions of the two intersection points that determine the beam direction. **d**, A scanning electron microscope micrograph of a fiber cross-section showing four electrodes in contact with a photoconductive, semiconducting glass core, surrounded by a protective polymer cladding.

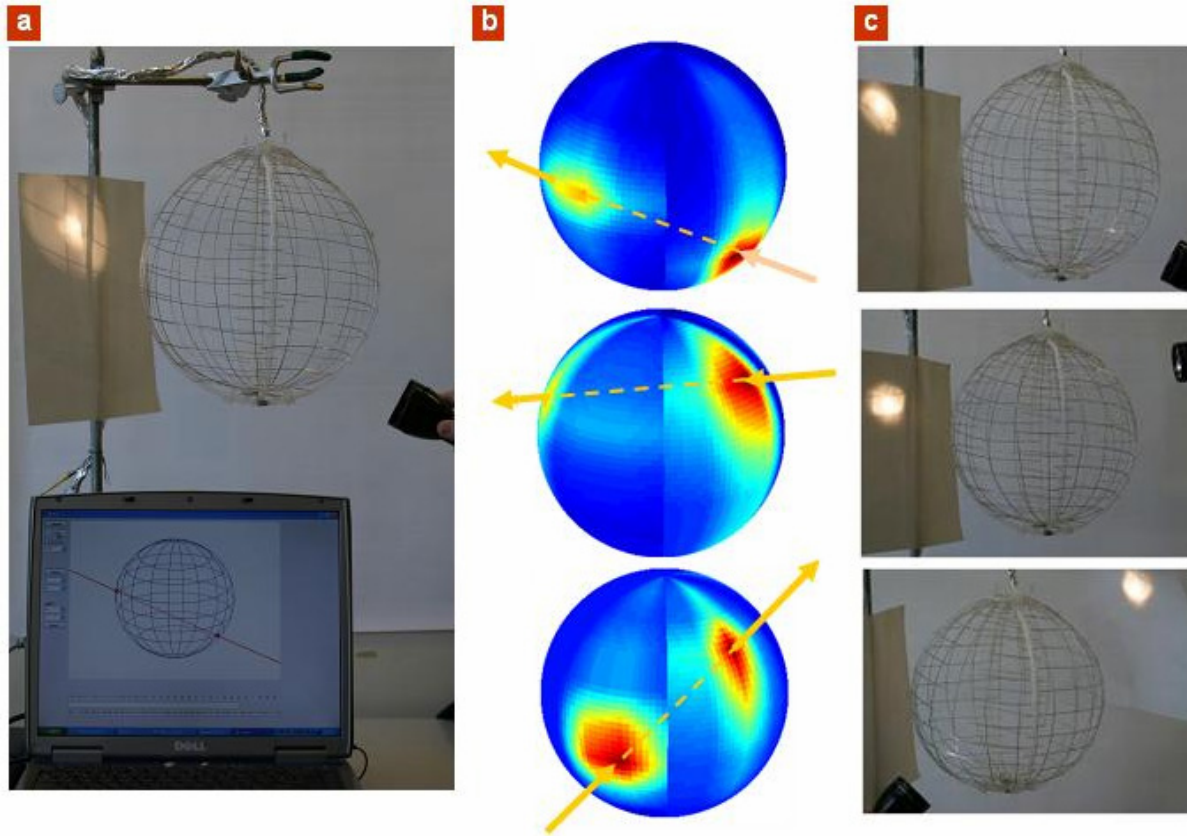


Figure 2 Omnidirectional light detection. **a**, A closed spherical fiber web is an omnidirectional photodetector which detects the direction of the beam throughout a solid angle of 4π . The meshgrid is sufficiently transparent to see through and for a beam of light to traverse unimpeded. **b**, The distribution of the electrical signals detected by the fibers for a light beam incident in three different directions. **c**, Photographs of the three beam trajectories that resulted in the signal distributions shown in **b**.

THERMAL FIBER GRIDS FOR SPATIALLY RESOLVED HEAT DETECTION ON LARGE AREAS

Academic and Research Staff

Mehmet Bayindir, Ayman F. Abouraddy, John D. Joannopoulos, and Yoel Fink

Sponsors

ISN, DARPA, the ONR, the US DOE and the NSF through the MIT MRSEC.

Thermal sensing yields important information about the dynamics of many physical, chemical, and biological phenomena. Spatially resolved thermal sensing enables failure detection in technological systems for which the failure mechanism is correlated with changes in temperature that are typically localized. Indeed infrared imaging systems have become ubiquitous for applications where visual contact could be made between the measured object and the camera lens. However, many critical applications do not lend themselves to radiative infrared imaging due to the subterranean nature of the monitored surface, or because of spatial constraints or cost considerations. The recent challenge of monitoring the skin temperature beneath the thermal tiles on the space shuttle represents a good example where high spatial resolution information is required on very large surface areas which cannot be performed using thermal imaging systems. Thus the problem of continuously monitoring and detecting a thermal excitation on very large areas (100m^2) with high resolution (1cm^2) is one that has remained largely unsolved.

We present a new methodology for measuring spatially resolved, temperature information of large areas bodies with high spatial resolution and low costs. Underlying our approach is a new fiber structure that senses heat along its entire length and generates an electrical signal. The fiber (cross-section is produced by thermal drawing of a macroscopic preform and combines three materials of widely disparate electrical and thermal properties. The semiconducting core is contacted by four Sn (Tin) metal conduits that are encapsulated in a protective polymer (polyethersulfone, PES) cladding. Hundreds of meters of flexible light-weight fibers can be produced from a single preform which makes the fiber intrinsically low cost. Four Sn electrodes run the entire length of the fiber in intimate contact with the glass, forming a metal-semiconductor-metal device structure. The electronic bandgap of this glass is small yielding a high electrical responsivity to small changes in temperature. In order to obtain spatially resolved information we assemble the fibers into a grid structure where the fibers are embedded in a fabric forming an 8×8 array with 1 cm separations. Each fiber is connected to an external circuit via the electrodes, and a signal proportional to the fiber resistance is digitized. A thermal map is reconstructed using these signals, and a localized excitation, such as the touch of a finger, is easily identified. This thermal map was corroborated by referencing it to a thermal image obtained by a thermal IR camera.

One intriguing application involves the thermal monitoring of the body of large aircraft or space shuttles by embedding such a fiber array on the skin and beneath the thermal tiles. An intense localized heat point is usually indicative of other faults and serves to predict failure. Another interesting application is in the thermal monitoring of patients or battlefield soldiers by their respective medical staff. The fiber arrays may be embedded in the patient's or soldier's clothing, a temperature map with resolution of relevance to physiological processes is produced and continuously fed to a remote station. High temperature chemical reactors and even vehicle tires fail via a spatially localized event which may manifest itself in terms of a thermal signature even prior to the actual failure. The low cost thermal grids will enable access to this information in real time and high resolution and can pave the way for more reliable, fault predictive technological systems.

References:

Published:

[1] T. Someya et al., "A Large-Area, Flexible Pressure Sensor Matrix with Organic Field-Effect Transistors for Artificial Skin Applications," *Proc. Natl. Acad. Sci.* 101: 9966 (2004).

[2] V. J. Lumelsky, M. S. Shur, and S. Wagner, "Sensitive Skin," *IEEE Sensors J.* 1: 41 (2001).

[3] M. Bayindir, F. Sorin, A. F. Abouraddy, J. Viens, S. D. Hart, J. D. Joannopoulos, and Y. Fink, "Metal-Insulator-Semiconductor Optoelectronic Fibres," *Nature* 431: 826 (2004).

Accepted for Publication:

[4] M. Bayindir, O. Shapira, D. Saygin-Hinczewski, J. Viens, A. F. Abouraddy, J. D. Joannopoulos, and Y. Fink, "Integrated Fibres for Self-Monitored Optical Transport," *Nature Materials*, forthcoming (2005).

[5] The 100's of meters of fiber was obtained from a macroscopic cylindrical preform, 31-mm in diameter and 20-cm long, which has the same fiber geometry. The preform was drawn in a three-zone vertical tube furnace with the top-zone temperature 195 °C and the middle-zone temperature 293 °C.

[6] The semiconducting core is an amorphous chalcogenide glass $\text{Ge}_{15}\text{As}_{25}\text{Se}_{15}\text{Te}_{45}$ that is characterized by enhanced stability against crystallization during fiber drawing, and has a glass transition temperature and viscosity that render it thermally compatible with a co-drawn polymer PES.

[7] The thermal activation energy of the glass was estimated as $\Delta E=0.495$ eV from the resistivity measurements.

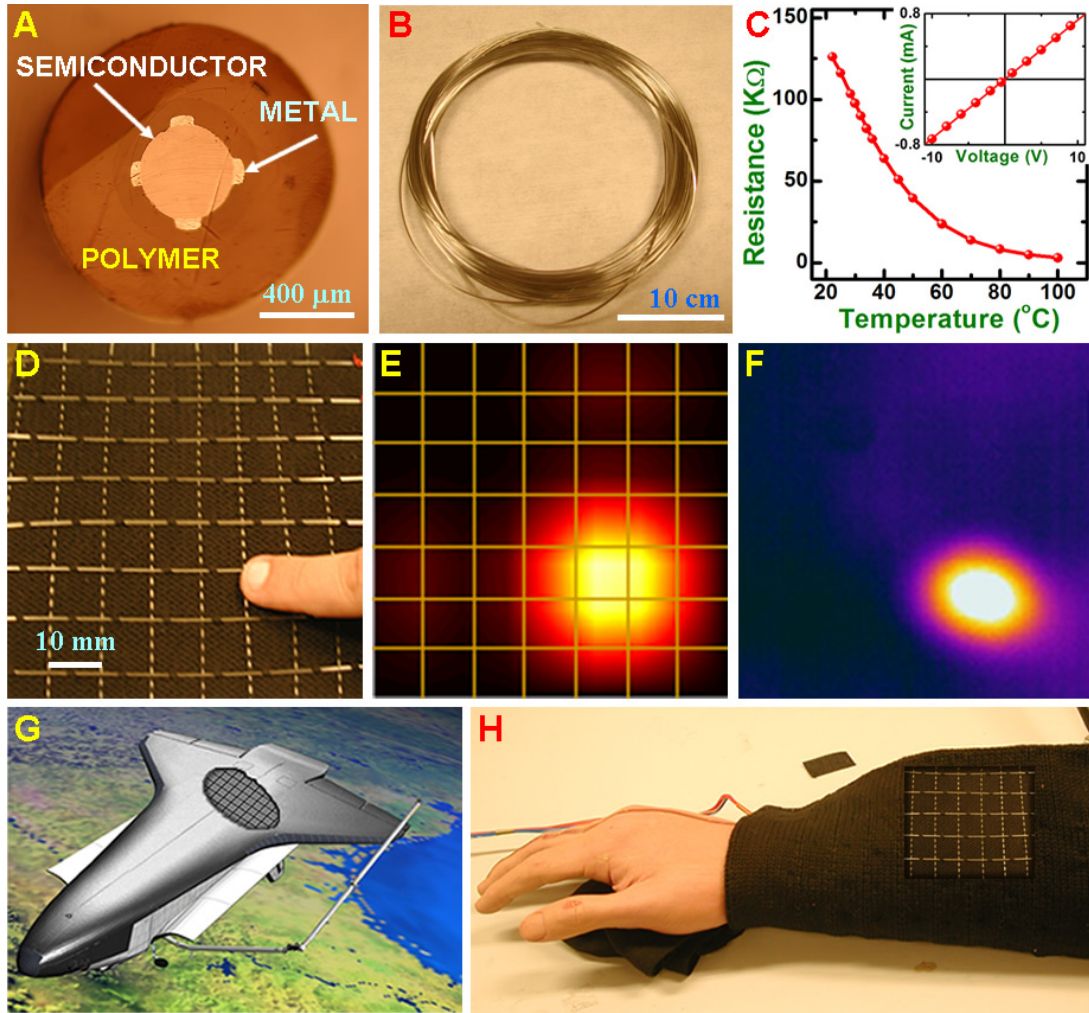


Fig. 1. (A) Micrograph of a thermal-sensing fiber cross-section (outer diameter is 1000 μm). (B) A 10-m long flexible fiber-based device is shown. (C) Resistance of 15 cm long fiber as a function of temperature. Inset shows the I-V curve of the fiber at 77 $^{\circ}\text{C}$. (D) An 8 \times 8 array of fibers is woven into a fabric and is touched by a finger. (E) A reconstructed temperature map produced using the electrical data collected from the fibers. (F) A thermal image of the fabric taken by an IR camera after the finger is removed. Thermal fabric covers (G) space shuttle surface (Photo credit/NASA) and (H) a patient's arm.

SURFACE-EMITTING POLYMER PHOTONIC BANDGAP FIBER LASERS

Academic and Research Staff

Ken Kuriki, Ayman F. Abouraddy, and Yoel Fink

Graduate Students

Gilles Benoit, Nicholas D. Orf, Jean F. Viens, Ofer Shapira, and Shandon D. Hart

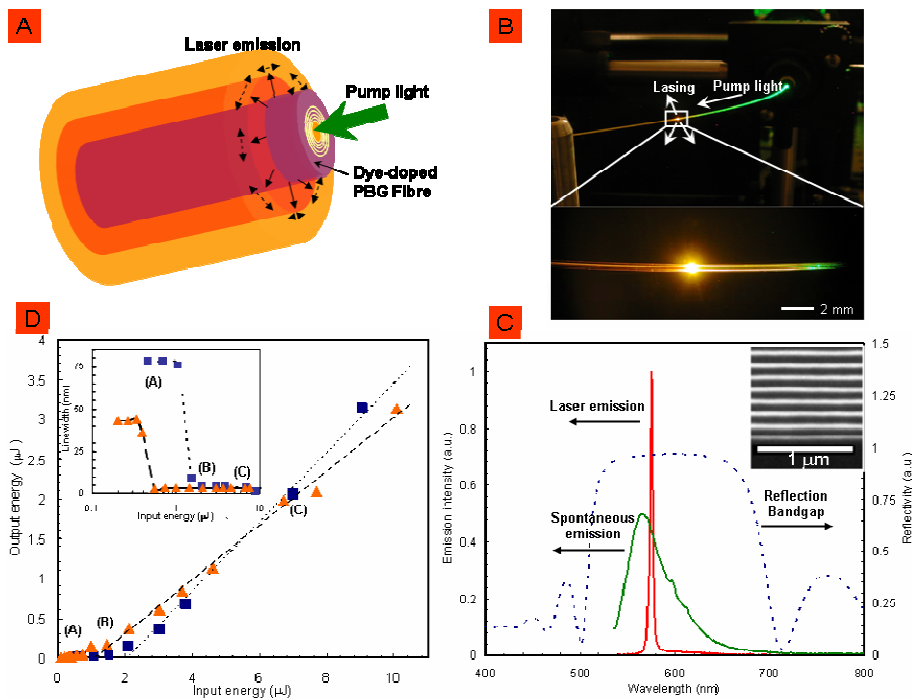
Visiting Graduate Student

Yuka Kuriki

Funding

AFRL

Optical lasing requires the confinement of a gain medium in a resonant cavity structure which provides the necessary optical feedback. Examples of such cavities range from the single-mode Fabry-Perot resonators used in vertical-cavity surface-emitting devices, to the large cavity structures associated with fiber lasers. Here we report on the design, fabrication and characterization of surface-emitting polymer fiber lasers which combine some of the key advantages and features of both vertical cavity and fiber lasers. A gain medium is placed in the hollow core of a cylindrical multilayer photonic bandgap fiber structure made of polyetherimide a high glass-transition-temperature polymer containing layers of As_2S_3 with individual layer thickness down to below 30nm. The characteristic shift of the photonic bandgap edges to higher frequencies with increased propagation vector enables the guidance of the high frequency optical pump along the fiber axis, while simultaneously acting as a transverse resonator at the lower lasing frequencies. The fibre-delivered axial excitation results in radially directed, uniform-surface laser emission from the entire fiber circumference surrounding the gain medium. High efficiency (~45%) and narrow-linewidth lasing at nine different wavelengths throughout the visible spectrum is demonstrated. The ability to remotely deliver surface-emitting lasing together with the high damage threshold, and superb mechanical properties characteristic of polyetherimide make this fiber laser an ideal candidate for non-invasive medical procedures, such as plaque removal from arteries, the activation of photodynamic therapies, and potentially for wearable multidirectional fabric displays.



A Schematic of the photonic bandgap fiber laser structure, pumping and emitted radiation geometry. The fiber laser emits light in the transverse direction (propagation vectors shown as solid arrows in upper panel) having a cylindrical wave front from an extended length of the fibre. The polarization of the wave front is transverse electric (TE), shown as dashed arrows in upper panel.

B A photograph of the R590-doped PBG fiber showing that the pump light at 532 nm (green) is being delivered in the hollow-core PBG fiber, and lasing at 576 nm (orange) occurs in the R590-core-doped region.

C Spontaneous and laser emission spectra from the R590-doped PBG fiber, and the calculated reflection spectrum of the fiber used for this dye. The fiber has a measured transmission bandgap at 515 nm (bandgap width is 5 %), and a reflection bandgap at 600 nm. Inset shows a cross-sectional SEM micrograph of the fibre and layer thicknesses down to 26.5 nm. The dye fluorescence spectrum lies in the reflection bandgap.

D Dependence of output energy on the input energy near threshold for the DCM (triangle) and the Ox725 (square)-doped PBG fibre lasers. Dotted and dashed lines are fits to the data to obtain laser-slope efficiencies. The laser-slope efficiencies of DCM and Ox725 are 34.0 % and 45.6 %, respectively. Inset, evolution of the spectral full-width at half-maximum as a function of input energy (on a logarithmic scale) for the DCM (triangle) and the Ox725 (square) -doped core PBG fibres. Points (A), (B), and (C) are associated with the Ox725 laser.